



Original Research Article

Voltammetric sensor for Nifedipine at woolen ball-shaped nanostructure modified glassy carbon electrode

Mohammad Mehdi Foroughi^{*1}, Shohreh Jahani², Soroush Rashidi³

^{1*} Department of Chemistry, Kerman Branch, Islamic Azad University, Kerman, Iran.

² Bam University of Medical Sciences, Bam, Iran.

³ Department of Civil Engineering, Islamic Azad University, Kerman, Iran.

Received: 2024-10-17

Accepted: 2024-12-17

Published: 2024-12-18

ABSTRACT

This work faces this challenge by the development of a novel electrochemical sensor via modifying a glassy carbon electrode (GCE) with woolen ball-shaped La³⁺/TiO₂ nanostructure (WB-S La³⁺/TiO₂-NS) for the detection of Nifedipine (NFP). Different characterization techniques indicate the successful synthesis of desired composite materials. Modified electrode exhibited higher peak current than the bare GCE, with excellent electrocatalytic ability to oxidize NFP, due to its higher conductivity, catalytic effect and synergistic effects between La³⁺ and TiO₂ nanostructure. Under optimized condition, differential pulse voltammograms (DPV) demonstrate that the oxidation peak current was proportional to its concentration in the range of 0.001–500.0 μM (R² = 0.9997) and low detection limit (0.43 nM). In addition, the modified electrode affirms good stability and reproducibility, making it simple, cost effective with high sensitivity. The results confirmed that making a composite is a key strategy for improving the physicochemical properties of TiO₂ nanostructure and that modifying electrode surfaces with novel composites can enhance the detection of NFP.

Keywords: Nifedipine, Voltammetry, Lanthanum, Nanostructure, Titanium dioxide.

*Corresponding author email address: Foroughi@iauk.ac.ir

Introduction

One of the leading causes of maternal and infant mortality, hypertension is a significant health concern in today's society [1-2]. Nifedipine (NFP, 2,6-dimethyl-4-(2-nitrophenyl)-1,4-dihydropyridine-3,5-dicarboxylate dimethyl ester) is one of the most used and prescribed drugs for the management and treatment of hypertension in various medical conditions and a series of cardiovascular disorders [3]. NFP is a medication that belongs to a class of drugs known as calcium channel blockers. NFP lowers blood pressure by blocking calcium from entering muscle cells around heart-feeding arteries [4,5]. However, NFP is poisonous in excess concentration and may have unpleasant moderate to severe consequences. Fatigue, dizziness, swelling in the legs, headache, coughing, and shortness of breath are among the symptoms that people often experience. The NFP residues can also enter the environment through biological fluids, becoming an emerging environmental pollutant [6]. Therefore, a cheap, sensitive, and straightforward NFP monitor is of tremendous value from a health perspective. Several approaches have been developed for the determination of NFP, including ultra-high pressure liquid chromatography-mass spectrometry (UHPLC-MS/MS), high-performance liquid chromatography, electrophoresis, and voltammetry [7-12]. Among them, using a portable and low-cost electrochemical approach offers a high dynamic range for clinical applications, and selectivity also allows for sufficient detection limits [13-15].

The combination of modern electrochemical methods and nanotechnology enables the development of strong and dependable electrical devices for efficient processes and detect analytes. Recent research has shown that obtaining nanomaterial fabricated electrodes with great sensitivity and even with individual nanoparticles (NPs) responding is possible. While an electrode modified with NPs offers significant benefits for electro-analysis, NPs generally play various functions in different electrochemical sensors [16].

Titanium dioxide nanoparticles (TiO_2 NPs) are one of the most widely applied nanoparticles. TiO_2 NPs occur in three different crystallographic forms: anatase and rutile (tetragonal) and, more rarely, brookite (orthorhombic). Among those three major polymorphs, anatase is extensively applied in commercial products due to its higher activity comparing to other forms, although rutile is the more stable form. Titanium dioxide nanostructures are widely used in electrochemical applications as well as in sensing and quantitation as an electrode modifier material [17-20].

In order to improve the performance of TiO₂ electrocatalytic, doping is used to a kind of modification method. Rare earth (RE) metal dopant can improve the activity of TiO₂, because RE elements have the 4f electron configuration, which reduce electron-hole pair recombination, leading to enhanced activity [21].

The present attempt was made to fabricate woolen ball-shaped La³⁺/TiO₂ nanostructure (WB-S La³⁺/TiO₂-NS), followed by characterization using techniques of X-ray diffraction (XRD), scanning electron microscopy (SEM) and energy-dispersive X-ray spectroscopy (EDX). A glassy carbon electrode (GCE) was then surface modified with WB-S La³⁺/TiO₂-NS (WB-S La³⁺/TiO₂-NS/GCE) to detect Nifedipine (NFP). The sensor was examined to detect NFP in real samples, the results of which highlighted appreciable recoveries, with good relative standard deviation (RSD), superior reproducibility and repeatability.

Experiments

Chemicals and devices

A SAMA 500 Electro analyzer was utilized to carry out all electrochemical tests. We employed a routine three-cell electrochemical system, including unmodified (bare) and modified glassy carbon working electrode, a reference electrode of Ag/AgCl (vs. 3.0 M KCl), and an auxiliary electrode of platinum wire. The solution pH was adjusted by a digital pH meter (Corning, Model: 140) equipped with a glass electrode (alongside an Ag/AgCl reference electrode, Model: 6.0232.100). A Philips analytical PC-APD X-ray diffractometer equipped with a graphite monochromatic Cu (α_1 , $\lambda_1=1.54056 \text{ \AA}$) and K α (α_2 , $\lambda_2=1.54439 \text{ \AA}$) radiation was recruited to record X-ray powder diffraction (XRD) to monitor the product organization. A KYKY and EM 3200 scanning electron microscopy (SEM) was used to explore the morphology of nanostructure. EDX spectroscopy is an example of a non-destructive instrument used for analysis, such as the analysis of chemical compounds. The buffered solution pH was adjusted by a digital Ion Analyzer 250pH meter (Corning) with precision of ± 0.001 .

Nifedipine (>99.0%) with very high purity belonged to Merck Company. Glacial acetic acid, titanium butoxide, lanthanum chloride, absolute ethanol and NaOH with analytical grade with no need for additional purification belonged to Sigma-Aldrich Company. Na₂HPO₄ (0.1 M) and NaH₂PO₄ (0.1 M) at various ratios were used to prepare the phosphate buffer solutions (PBS). H₃PO₄ (1.0 M) and/or NaOH were used to adjust the solution pH.

Fabrication of Woolen ball-shaped La³⁺/TiO₂ nanostructure (WB-S La³⁺/TiO₂-NS)

Titanium butoxide (1 mL) and lanthanum chloride (0.02 g) were appended drop-by-drop into glacial acetic acid (30 mL) while stirring continuously for 10 min at an ambient temperature to obtain white suspension, which was then positioned in a 150-mL Teflon-lined autoclave at 140 °C for 12 h. The appeared white product was gathered by centrifugation, rinsed several times initially with Milli-Q and then with ethanol, and finally dried in a 60-°C oven overnight to obtain as as-fabricated WB-S La³⁺/TiO₂-NS.

Synthesis of WB-S La³⁺/TiO₂-NS electrode

Considering the significance of electrode fabrication in electrochemistry, first the glassy carbon electrode (GCE) surface was completely rinsed with water to get rid of possible impurities. The following protocol was implemented to prepare the WB-S La³⁺/TiO₂-NS/GCE. First, WB-S La³⁺/TiO₂-NS suspension was synthesized by dispersing WB-S La³⁺/TiO₂-NS (1 mg) in double distilled water (1 mL) under 30-min sonication. Then, WB-S La³⁺/TiO₂-NS suspension (6 µL) was drop coated on the surface of GCE and dried at the ambient temperature.

Preparation of real specimens

NFP tablets (labeled 10 mg NFP/tablet) were powdered, 10 mg of which was then appended into water (25 mL) and exposed to ultra-sonication. A certain volume of the obtained solution alongside phosphate buffer solution (PBS, pH 7.0) was water-diluted in a 10-mL voltammetric flask. The achieved solution was applied for the NFP analysis.

Blood samples gathered in heparinized test tubes underwent a centrifugation for 10 min at 3000 rpm to separate the plasma, which was then refrigerated for next testing. Acetonitrile was used to deproteinate the plasma samples, so that the acetonitrile (2 mL) was appended to plasma and the mixture underwent a centrifugation for 10 min at 2000 rpm. The supernatant was evaporated in a conical flask to dryness in exposure to nitrogen flow. The dry residue was diluted with PBS (pH 7.0) and poured into the voltammetric cell (20 mL) for analysis with no need for pretreatment. The NFP were quantified in the samples according to standard addition method.

Urine specimens sampled from healthy subjects were analyzed to determine possible traces of NFP. After that, the samples were diluted 50 times with PBS to avoid the matrix effect of valid samples.

Results and discussion

Determination of WB-S La³⁺/TiO₂-NS characteristics

The XRD patterns captured from pure TiO₂ (curve a) and La³⁺/TiO₂ nanostructure (curve b) are presented in Figure 1. Crystal structures of pure TiO₂ and nanostructured La³⁺/TiO₂ were mainly composed of anatase phase (JCPDS 21-1272). The anatase peaks appeared at 25.371, 38.51, 48.211, and 54.101 were related to (101), (004), (200), and (105) planes, sequentially. There were no distinct peaks (La³⁺ metal, La₂O₃) following the integration of La dopants into the TiO₂ nanostructure probably due to inadequate sensitivity of XRD analysis in sensing traces of La dopants within the TiO₂ nanostructure [22]. The shift of diffraction peaks and the change in full width at half maximum for the La³⁺/TiO₂ nanostructure, anatase phase may be attributed to the integration of La³⁺ dopants into the TiO₂ lattice.

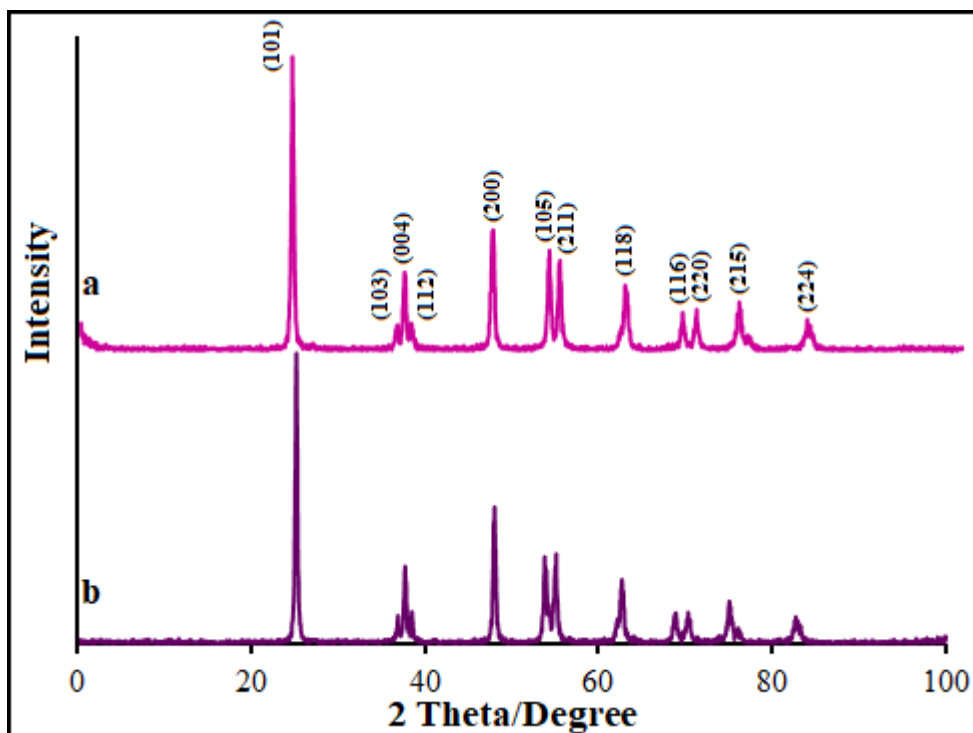


Figure 1. XRD pattern of a) A-L TiO₂ NF and b) WB-S La³⁺/TiO₂-NS.

The FE-SEM images (Figure 2a, b) were applied to explore the morphology of Anastasia-like TiO₂ nanoflowers (A-L TiO₂ NF), the findings of which clarified a spherical hierarchical architecture with thin and long two-dimensional nanosheets (i.e., ~10-nm petals, forming A-L TiO₂ NF) protruding from the center of the three-dimensional nanoflowers (2-6 μm in diameter, the mean diameter of 4.5 μm). Based on Figure 2c, as-produced woolen ball-shaped La³⁺/TiO₂ nanostructures (WB-S La³⁺/TiO₂ NS) consisted of large-scale woolen ball-flower structures

(1.8 to 2.4 μm in diameter). SEM images with high magnification from WB-S $\text{La}^{3+}/\text{TiO}_2$ NS (Figure 2d) present two-dimensional well-ordered and -oriented nanoplates (20-30 nm) for WB-S $\text{La}^{3+}/\text{TiO}_2$ NS to form woolen ball-flower structures. The FE-SEM images exhibits the impact of La ion content on the TiO_2 morphology.

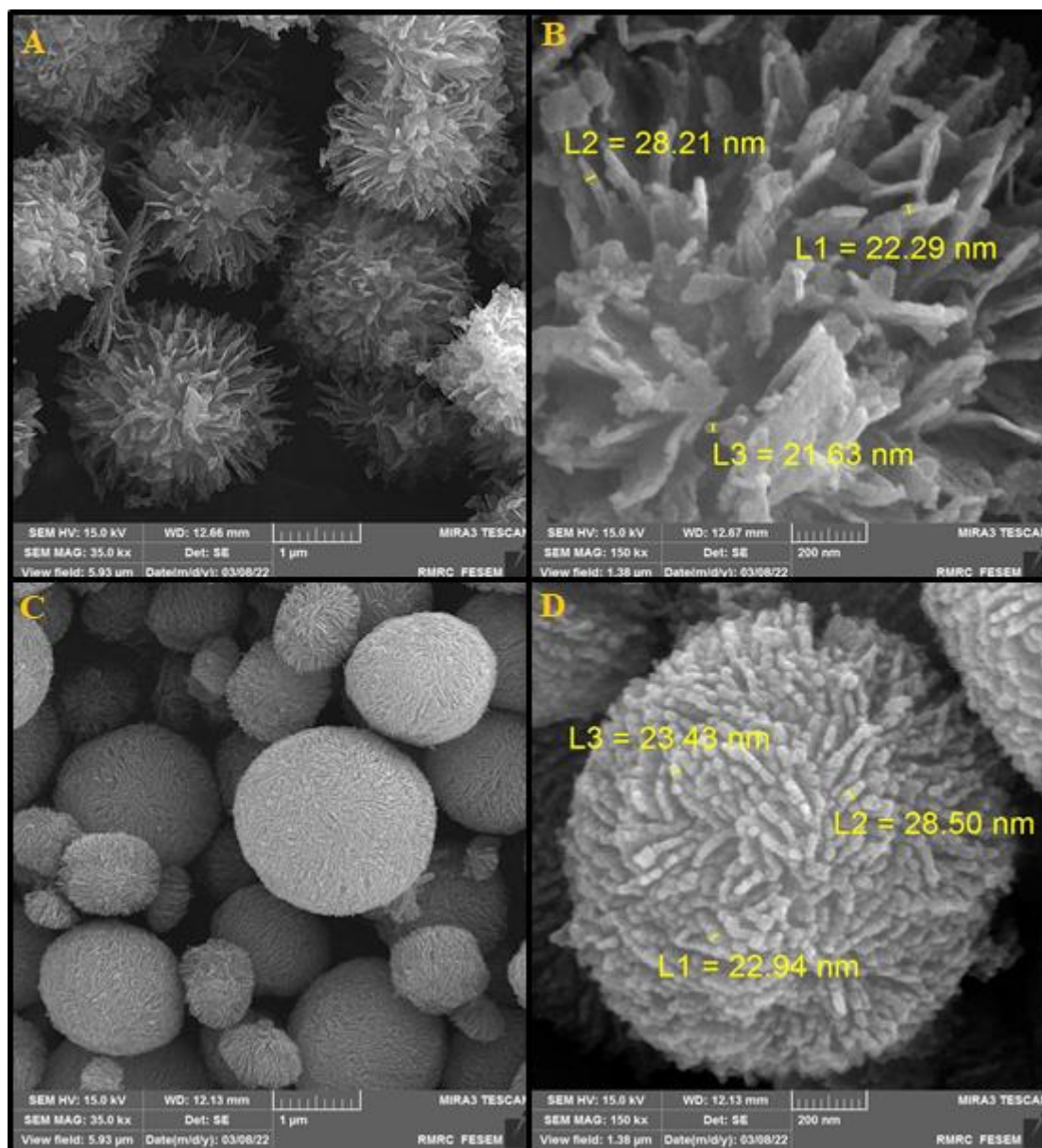


Figure 2. (A) FESEM image (B) High resolution FESEM image of A-L TiO_2 NF. (C) FESEM image (D) High resolution FESEM image of WB-S $\text{La}^{3+}/\text{TiO}_2$ -NS.

The EDS pattern (Figure 3) shows that the woolen ball-flower products are built of Ti, O and La elements without any impurity. The distribution of Ti, O and La was confirmed by the elemental mapping.

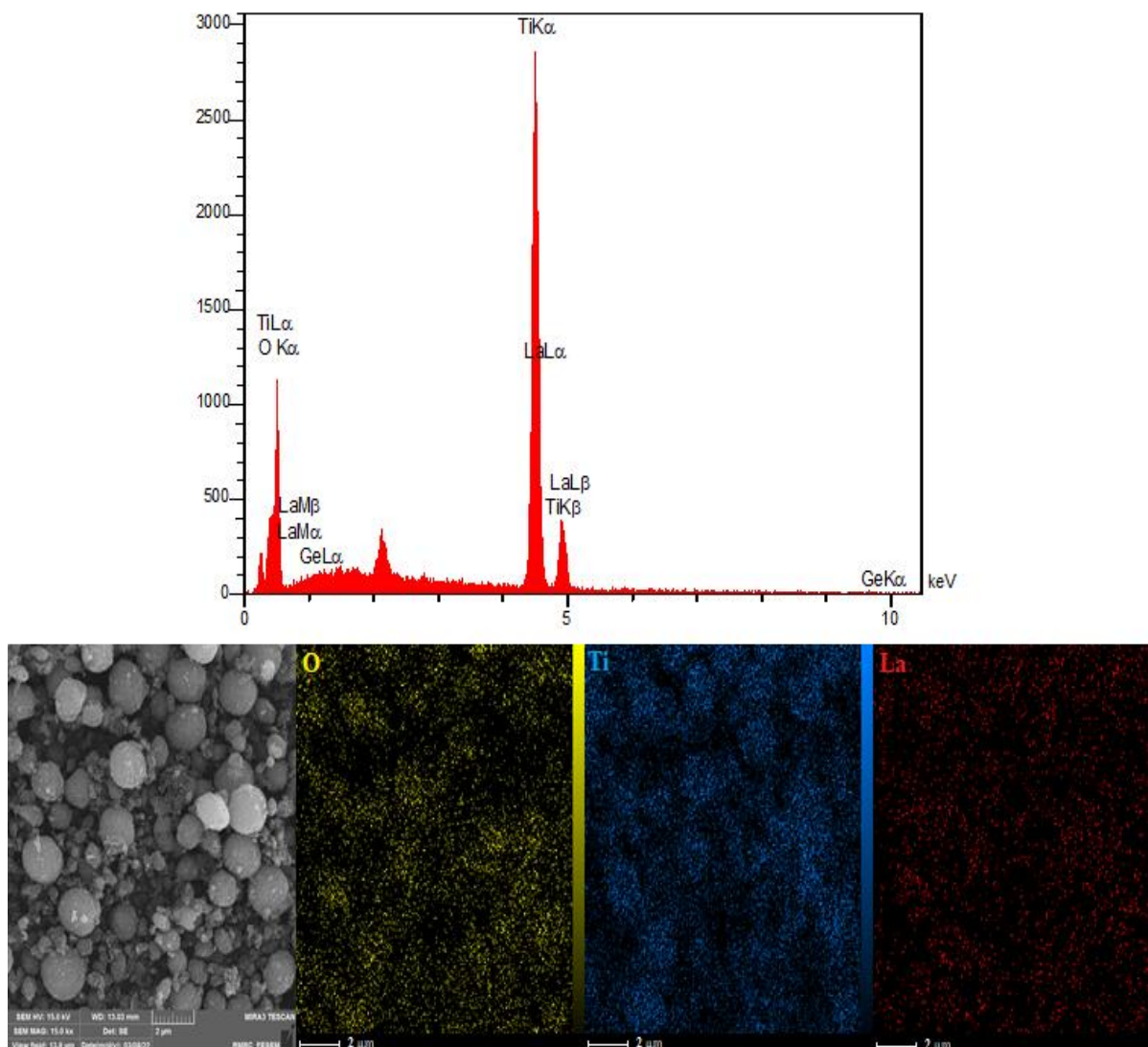


Figure 3. EDX spectra and elemental mapping of WB-S La³⁺/TiO₂-NS.

Electrochemical behavior of NFP on the modified electrode

The electrochemical response of NFP (30.0 μM) was recorded in PBS (pH 7, 0.1 M) at scan rate of 50 mV/s using the CVs on bare GCE (curve a), A-L TiO₂ NF/GPE (curve b) and WB-S La³⁺/TiO₂-NS/GCE (curve c) (Figure 4). The peak current of NFP oxidation had a significant elevation approximately 1.92 and 9.4 times higher on the WB-S La³⁺/TiO₂-NS/GCE than that on the A-L TiO₂ NF/GCE and bare GCE, sequentially. The peak potentials of them were switched to less positive side with WB-S La³⁺/TiO₂-NS/GCE than A-L TiO₂ NF/GCE and bare GCE, sequentially. The peak potential was seen for NFP at -780 mV on the WB-S La³⁺/TiO₂-NS/GCE and A-L TiO₂ NF/GCE, at -860 mV on a bare GCE, sequentially, highlighting a platform role of both La³⁺ and TiO₂ electrodes for the NFP oxidation.

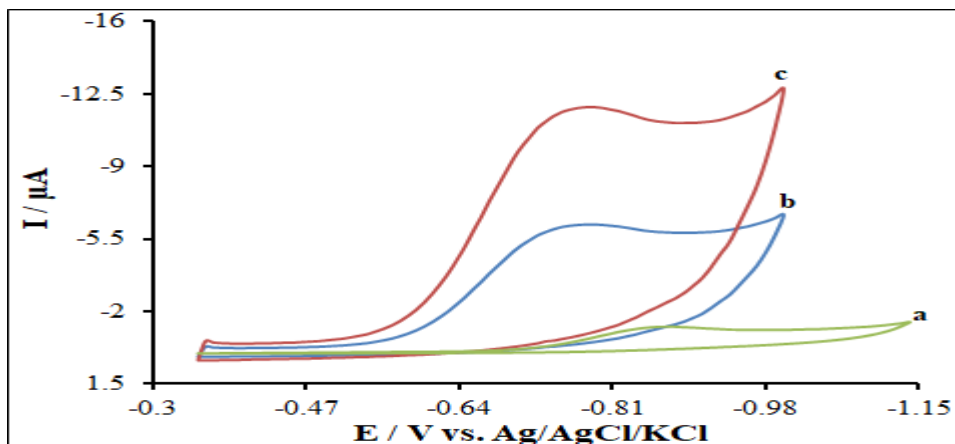


Figure 4. CVs of NFP (30.0 μM) at a) bare GCE, b) A-L TiO_2 NF/GCE and c) WB-S $\text{La}^{3+}/\text{TiO}_2$ -NS/GCE in 0.1 M PBS (pH=7.0).

Further, we investigated the influence of the scan rate of the modified electrode system with respect to the oxidation of NFP (5.0 μM) in the changes of the scan rate, as shown in Figure 5. There was an elevation in the NFP anodic currents when the scan rate boosted to 500 from 10 mV/s. According to the inset, the liner curves of NFP anodic currents against the scan rate square root ($v^{1/2}$) confirms diffusion-controlled process for the oxidation of NFP on the WB-S $\text{La}^{3+}/\text{TiO}_2$ -NS/GCE.

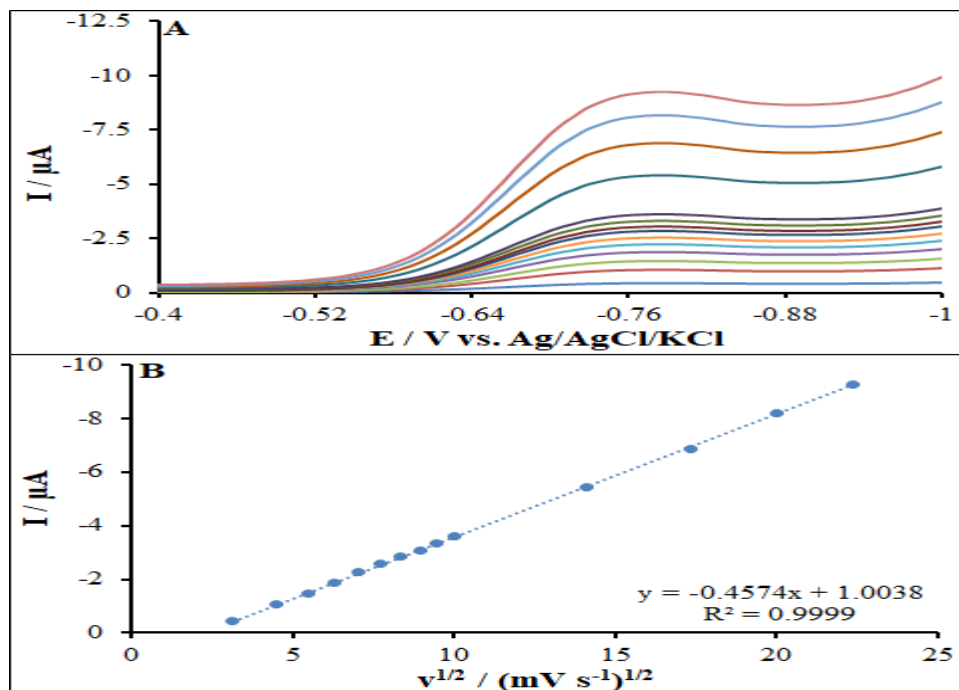


Figure 5. (A) CVs of WB-S $\text{La}^{3+}/\text{TiO}_2$ -NS/GCE in pH 7.0 in the presence of NFP (5.0 μM) at various scan rates (from inner to outer curve): 10, 20, 30, 40, 50, 60, 70, 80, 90, 100, 200, 300, 400 and 500 mV/s. (B) The plots of peak currents vs. $v^{1/2}$ of NFP.

Chronoamperometric determinations

The chronoamperometric determination was carried out by altering the level of NFP in PBS at the potentials of 830 mV set for WB-S La³⁺/TiO₂-NS/GCE (Figure 6A).

The current response (I) for diffusion-controlled process of electroactive NFP was explained by Cottrell's equation (Eq. 1) [23]:

$$I = nFAD^{1/2}C_b\pi^{-1/2}t^{-1/2} \quad (\text{Eq. 1})$$

Where, D (cm²s⁻¹) stands for the diffusion coefficient of studied species, F for the Faraday constant (96485 CM), C_b for the bulk content of studied species (mol cm⁻³), n for the number of electrons transferred (2), and A for electrode surface area (cm²). Data revealed a linear curve from the raw chronoamperometric traces for variable NFP levels by diagramming I versus t^{-1/2} (Figure 6B). Then, the slope of the straight lines versus the concentrations of NFP in Figure 6C was drawn. Next, the estimated diffusion coefficient was 1.99×10⁻⁶ cm²s⁻¹ for NFP.

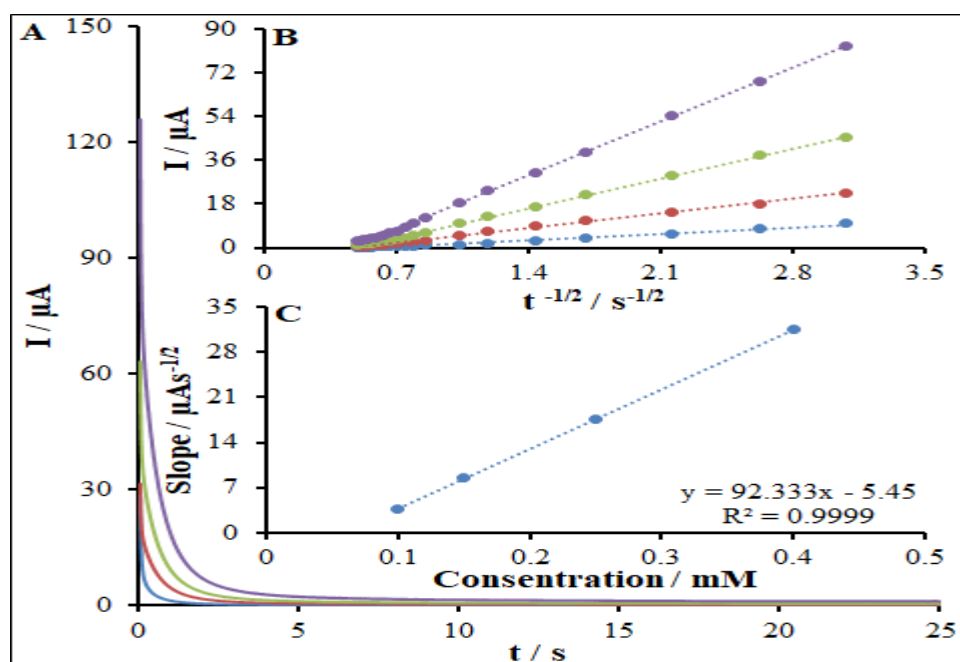


Figure 6. (A) Chronoamperograms obtained at WB-S La³⁺/TiO₂-NS/GCE in 0.1 M PBS (pH 7.0) for different concentration of NFP. The numbers 1–4 correspond to: 0.1, 0.15, 0.25 and 0.4 mM of NFP.

(B) Plots of I vs. t^{-1/2} obtained from chronoamperograms 1-4 for NFP. (C) Plot of the slope of the straight lines against NFP concentration, respectively.

Detection of NFP

The DPVs (Figure 7) were captured for variable NFP levels in PBS (pH=7, 0.1 M) to determine the performances of WB-S La³⁺/TiO₂-NS/GCE for the detection of NFP. There was an elevation in the peak currents when the solution level of NFP increased whereas the peak

potentials of NFP were constant. The relevant liner standard plots were achieved in the ranges of 0.001 to 500.0 μM for NFP. Linear regression equation of standard graphs and correlation coefficient of NFP are given as follows:

$$I_{\text{NFP}} = -0.0398 C_{\text{NFP}} + 0.0783, R^2 = 0.9997 \quad (\text{Eq. 2})$$

The limit of detection (LOD) of NFP was determined on the basis of five determinations of the blank noise standard deviation ($n = 5$) on the basis of reported method, using the equation $3S_b/m$; where, m stands for the slope of the standard plot and S_b for the standard deviation, which was 0.43 μM . The narrow LOD of NFP with as-fabricated nanocomposite suggests good work and efficient analysis of WB-S $\text{La}^{3+}/\text{TiO}_2\text{-NS/GCE}$.

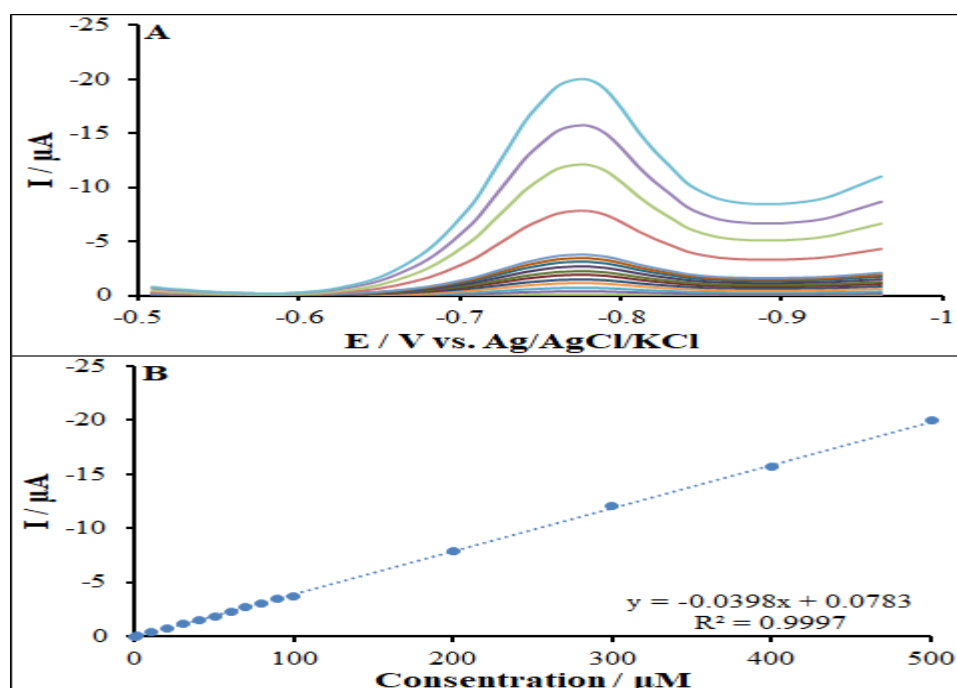


Figure 8. (A) DPVs of the NFP at the WB-S $\text{La}^{3+}/\text{TiO}_2\text{-NS/GCE}$ in PBS (pH 7.0) at the scan rate of 50 mV s^{-1} , respectively, Concentrations from inner to outer of curves: 0.001, 0.1, 1.0, 10.0, 20.0, 30.0, 40.0, 50.0, 60.0, 70.0, 80.0, 90.0, 100.0, 200.0, 300.0, 400.0 and 500.0 μM . (B) Plots of I vs. Concentrations of NFP.

Stability and reproducibility of the modified electrode

The WB-S $\text{La}^{3+}/\text{TiO}_2\text{-NS/GCE}$ was examined for the reproducibility by studying the current behavior of NFP with five electrodes constructed by the same ways. According to the findings, the relative standard deviation (RSD) of the electrodes was 2.92% for NFP. The WB-S $\text{La}^{3+}/\text{TiO}_2\text{-NS/GCE}$ was also examined for the stability to NFP during four weeks. There was a reduction in the currents responses by 2.57% for NFP. Accordingly, the as-developed WB-S $\text{La}^{3+}/\text{TiO}_2\text{-NS/GCE}$ possessed a commendable reproducibility long stability for sensing NFP,

so that it can show analytical application for detection of the NFP for over one month with no noticeable influence in its activity.

Interference analysis

We evaluated the impacts of possible interferants present in bio-fluids or pharmaceutical formulations for concurrent detection of 10.0 μM of NFP. The greatest level of the possible interferants, which causes an error of <5%, was regarded as the tolerance limit. According to the findings, 2000 times the level of glucose, phenylalanine, alanine, sucrose and methionine, and 600 times the content of histidine and glycine had no impact on the NFP oxidation currents, underlining the successful performance of the as-fabricated sensor for concurrent detection of NFP.

Real sample testing

Therefore, we employed the standard addition method for evaluating the potential of the WB-S $\text{La}^{3+}/\text{TiO}_2\text{-NS}/\text{GCE}$ as one of the novel analytical approaches to determine NFP in the real samples (Table 1). According to the table, the recoveries from 98.6 to 102.0% verified the major ability of the WB-S $\text{La}^{3+}/\text{TiO}_2\text{-NS}/\text{GCE}$ as one of the modern nano-sensors to detect NFP in the real samples.

Table 1. Determination of NFP in NFP tablets, human blood serum and urine samples. All the concentrations are in μM (n=5).

Sample	Spiked	Found	Recovery (%)	R.S.D. (%)
NFP tablets	0.0	2.1	-	2.2
	10.0	12.2	100.8	1.7
	15.0	17.3	101.2	2.8
Human blood serum	0.0	0.0	-	-
	7.5	7.4	98.6	2.4
	12.5	12.2	97.6	1.9
Urine	0.0	0.0	-	-
	15.0	15.2	101.3	3.3
	25.0	24.9	99.6	2.5

Conclusion

The current investigation involved the examination of the electrochemical characteristics of NFP through the utilization of an electrochemical sensor constructed with WB-S $\text{La}^{3+}/\text{TiO}_2\text{-NS}$. Compared to bare GCE and A-L $\text{TiO}_2\text{ NF}/\text{GCE}$, WB-S $\text{La}^{3+}/\text{TiO}_2\text{-NS}/\text{GCE}$ achieved good current sensitivity for NFP, with modified electrode good current responsiveness and stability were successfully attained a low detection limit. The phenomenon of electrode process is

governed by diffusion, and the determined quantities for Limit of Detection (LOD) and Limit of Quantification (LOQ) yielded values of 0.43 nM and 1.44 nM respectively. Additionally, the linear correlation coefficient for NFP was determined to be $R^2 = 0.9997$. Likewise, a good recovery results were attained when the WB-S $\text{La}^{3+}/\text{TiO}_2\text{-NS/GCE}$ was used to detect the NFP in real samples.

References

- [1] V. Brovkovich, L. Kalinowski, R. Muller-Peddinghaus, T. Malinski, *Hypertension.*, 37, 34-39 (2001).
- [2] J. Scremin, E.R. Sartori, *Can. J. Chem.*, 96, 1 (2018).
- [3] M.D.H. Wirzal, P. Sathishkumar, L.A. Alshahrani, A.R.M. Yusoff, F.L. Gu, M.S. Qureshi, M. Khalid, F.M. Khokhar, *Chem. Pap.*, 75, 681 (2021).
- [4] S. Kulkarni, M. Glover, V. Kapil, S.M.L. Abrams, S. Partridge, T. McCormack, P. Sever, C. Delles, I.B. Wilkinson, *J. Hum. Hypertens.*, 2022, 1 (2022).
- [5] T. Firoz, L.A. Magee, K. MacDonell, B.A. Payne, R. Gordon, M. Vidler, P. von Dadelszen, *BJOG Int. J. Obstet. Gynaecol.*, 121, 1210 (2014).
- [6] M. Khairy, A.A. Khorshed, F.A. Rashwan, G.A. Salah, H.M. Abdel-Wadood, C.E. Banks, *Sensor. Actuator. B Chem.*, 252, 1045 (2017).
- [7] C.W. Thorstensen, P.E. Clasen, S. Rognstad, R. Haldsrud, S. Føreid, T. Helstrøm, O. U. Bergland, L.V. Halvorsen, A. Aune, E. Olsen, K.M. Brobak, A. Høieggen, I. Gustavsen, A.C.K. Larstorp, C.L. Sjøraas, M.S. Opdal, *J. Pharm. Biomed. Anal.*, 219, 114908 (2022).
- [8] S. Ahmed, A. Alqurshi, A.M.I. Mohamed, *Talanta*, 184, 296 (2018).
- [9] L. Zeng, X. Wu, Y. Li, D. Lu, C. Sun, *Anal. Methods*, 7, 543 (2015).
- [10] P. Sundaresan, R. Karthik, S.M. Chen, J. Vinoth Kumar, V. Muthuraj, E. R. Nagarajan, *Ultrason. Sonochem.*, 53, 44 (2019).
- [11] R.R. Gaichore, A.K. Srivastava, *Sens. Actuators B Chem.*, 188, 1328 (2013).
- [12] J.P. Winiarski, M.R. de Barros, G.S. Wecker, G.R. Nagurniak, R.L.T. Parreira, R. F. Affeldt, R.A. Peralta, C.L. Jost, *J. Mater. Chem. C*, 8, 6839 (2020).
- [13] T. Iranmanesh, Sh. Jahani, M.M. Foroughi, M. Shahidi Zandi, H. Hasani Nadiki, *Anal. Methods*, 12, 4319 (2020).
- [14] S. Ershad, S. Dadmanesh, M. Hosseinzadeh, *Int. J. New. Chem.*, 11, 58 (2024).
- [15] N. Farvardin, Sh. Jahani, M. Kazemipour, M.M. Foroughi, *Anal. Methods*, 12, 1767 (2020).

- [16] S. Ershad, S. Jalali, M. Hosseinzadeh, *Int. J. New. Chem.*, 11, 113 (2024).
- [17] D.M. Stankovi'c, E. Mehmeti, J. Zava'snik, K. Kalcher, *Sensors Actuators, B Chem.*, 236, 311 (2016).
- [18] H. Abe, Y. Kimura, T. Ma, D. Tadaki, A. Hirano-Iwata, M. Niwano, *Sensors Actuators, B Chem.*, 321, 128525 (2020).
- [19] M. Arvand, N. Ghodsi, M.A. Zanjanchi, *Biosens. Bioelectron.*, 77, 837 (2016).
- [20] K. Murtada, S. Jodeh, M. Zougagh, 'A. Ríos, *Electroanalysis*, 30, 969 (2018).
- [21] H. Liu, M.Y. Wang, Y. Wang, Y.G. Liang, W.R. Cao, Y. Su, *J. Photochem. Photobiol. A: Chem.*, 223, 157 (2011).
- [22] J. Liu, X. Li, *Phys. Lett. A*, 378, 405 (2014).
- [23] A.J. Bard, L.R. AJ. Faulkner, *Electrochemical Methods: Fundamentals and Applications*, second ed., Wiley, New York (2001).

HOW TO CITE THIS ARTICLE

Mohammad Mehdi Foroughi; Shohreh Jahani; Soroush Rashidi. "**Voltammetric sensor for Nifedipine at woolen ball-shaped nanostructure modified glassy carbon electrode**", *International Journal of New Chemistry*, 2025; 12(4), 540-552. doi: 10.22034/ijnc.2024.2022678.1376.